Mineralogical Magazine (2023), **87**, 233–240
doi:10.1180/mgm.2023.1

Article

Synthesis of Fe-deficient eudialyte analogues: Relationships between the composition of the reaction system and crystal-chemical features of the products

Tatiana N. Kovalskaya[1]*, Vera N. Ermolaeva[1,2], Nikita V. Chukanov[3], Dmitry A. Varlamov[1,3], Georgy A. Kovalskiy[1], Egor S. Zakharchenko[1], Georgy M. Kalinin[1,]† and Korney D. Chaichuk[1]

[1]D.S. Korzhinskii Institute of Experimental Mineralogy the Russian Academy of Sciences (IEM RAS), 4 Academician Ossipyan str., Chernogolovka, Moscow District, 142432 Russia; [2]Vernadsky Institute of Geochemistry and Analytical Chemistry the Russian Academy of Sciences (GEOKHI RAS), 19 Kosygin str., Moscow, 119991 Russia; and [3]Institute of Problems of Chemical Physics the Russian Academy of Sciences (IPCP RAS) Ac. Semenov avenue 1, Chernogolovka, Moscow region, 142432 Russia

Abstract

Eudialyte-related compounds have been synthesised hydrothermally at $T = 600°C$ and $P = 2$ kbar from a stoichiometric mixture of Na_2CO_3, CaO, Fe_2O_3, $ZrOCl_2$ and SiO_2 using the Na:Ca:Fe:Zr:Si ratios corresponding to the eudialyte end-member $Na_{15}Ca_6Fe_3Zr_3Si(Si_{25}O_{73})(OH)Cl_2{\cdot}H_2O$, in the presence of 1 M aqueous solutions of NaCl and NaF. The synthesis was carried out in platinum ampoules over 10 days. Natural raslakite (a Ca-deficient member of the eudialyte group) was used as a seed and added in amounts corresponding to 2 wt.% of the whole charge. The products were characterised by powder X-ray diffraction, IR and Raman spectroscopy, morphological features, and electron probe microanalyses. In experiments with NaCl, almost pure eudialyte-type compounds were obtained. Synthesis in the presence of a NaF solution resulted in the formation of a F-dominant eudialyte-type compound related to raslakite as the main product and aegirine, vlasovite and lalondeite as by-products. All synthesised eudialyte-type compounds are Zr-rich and Fe-deficient, similar to eudialyte-group minerals from hyperagpaitic rocks related to foyaites. The increased NaCl contents in the reaction system results in increased Ca content in the synthesised eudialyte-related compounds. The crystal-chemical formulae of the synthesised eudialyte-type compounds are derived based on general regularities established earlier for eudialyte-group minerals.

Keywords: eudialyte, hydrothermal synthesis, crystal chemistry, peralkaline complexes

(Received 15 August 2022; accepted 3 January 2023; Accepted Manuscript published online: 13 January 2023; Associate Editor: Katharina Pfaff)

Introduction

In recent years, eudialyte-group minerals (EGM) have attracted increased attention. On the one hand as typical accessory (and sometimes rock-forming) minerals of agpaite complexes they are relatively widespread: numerous discoveries have been made in dozens of alkaline complexes. On the other hand, unlike most other rock-forming minerals, EGM have the ability to concentrate a number of rare elements (Zr, Hf, Nb and rare earth elements), and are therefore of practical interest as a potential source of these elements. However, the most interesting feature of eudialyte-related minerals is the unique complexity and variability of their crystal structures within one overall structure motif. The EGM are a very effective model on which many crystal-chemical, geochemical and genetic regularities have been established (Rastsvetaeva *et al.*, 2012; Rastsvetaeva *et al.*, 2020; Rastsvetaeva and Chukanov, 2020; Chukanov *et al.*, 2020). The EGM are trigonal, with space groups $R3m$, $R\bar{3}m$ or $R3$, and the unit-cell parameters $a = 14.1–14.2$ and $c = 30.0–30.8$ or ~60 Å (the c parameter is doubled in samples with modular structures). The crystal structures of EGM are based on a heteropolyhedral framework composed on Si_3O_9 and Si_9O_{27} rings of tetrahedra, $M1_6O_{24}$ rings of edge-sharing octahedra connected *via* $M2O_{4–7}$ polyhedra and isolated ZO_6 octahedra. Various cations with charges from +1 to +6 and coordination numbers 4 or 6 can occur at the *M*3 and *M*4 sites situated near the centres of the Si_9O_{27} rings. Large extra-framework cations occupy the *N*1–5 sites. Different extra-framework anions and water molecules occur at the O′, *X*1 and *X*2 sites. In most cases, in EGM so-called 'blocky' isomorphism is realised when one group of atoms and ions is replaced by another one, which is accompanied by a change in the valence state and/or coordination numbers of cations. In reality, the *N*1–5 and *M*2–4 sites do not have fixed positions but are micro-regions in which blocky isomorphism is realised. For these sites, splitting is very typical.

The general formula of EGM is ($Z = 3$; see Johnsen *et al.*, 2003): $N1_3N2_3N3_3N4_3N5_3M1_6M2_{3–6}M3M4Z_3(Si_{24}O_{72})O'_{4–6}X1X2$ where: $N1–5 = Na$, K, H_3O^+, Ca, Mn^{2+}, Sr, Ba and rare earth elements (*REE*); $M1 = Ca$, Mn^{2+}, Fe^{2+}, *REE*, Na and Sr; $M2 = Mn^{2+}$,

---

*__Author for correspondence:__ Tatiana N. Kovalskaya, Email: tatiana76@iem.ac.ru

†Deceased

Cite this article: Kovalskaya T.N., Ermolaeva V.N., Chukanov N.V., Varlamov D.A., Kovalskiy G.A., Zakharchenko E.S., Kalinin G.M. and Chaichuk K.D. (2023) Synthesis of Fe-deficient eudialyte analogues: Relationships between the composition of the reaction system and crystal-chemical features of the products. *Mineralogical Magazine* **87**, 233–240. https://doi.org/10.1180/mgm.2023.1

Fe^{2+}, Fe^{3+}, Na, Zr, Ta, Ti, K and H_3O^+; *M*3 and *M*4 = Si, S, Nb, Ti, W and Na; *Z* = Zr, Ti and Nb; O′ = O, OH or H_2O; *X*1 and *X*2 = F, Cl, H_2O, OH, CO_3 and SO_4.

Currently, the eudialyte group contains 31 mineral species approved by the Commission on New Minerals, Nomenclature and Classification of the International Mineralogical Association. Of these, 18 minerals were discovered in agpaitic rocks of three large alkaline massifs (Khibiny, Lovozero and Kovdor) located on the Kola Peninsula, Russia, and most of the remaining EGM were also identified there as accessory components of pegmatites.

From the petrological point of view, three main kinds of EGM can be distinguished. Type 1 is most common. This includes eudialyte *s.s.* and dominates in the Khibiny massif, and can be termed the Khibiny type. In this type, univalent cations (Na and in some cases subordinate K) prevail at the *N* sites, the *M*1 site is occupied mainly with Ca (typically, 5 to 6 Ca atoms per formula unit, apfu), the *M*2 site contains bivalent cations (Fe^{2+}, rare Mn^{2+}) and the *M*3 and *M*4 sites are occupied predominantly by Si. Thus, homovalent isomorphism is typical for the Khibiny-type EGM.

Type 2 (Lovozero type) is a Ca deficient EGM variety (with <5 Ca apfu) typical of peralkaline rocks of the Lovozero massif. In these minerals, Ca is partly substituted by Mn^{2+} and/or Fe^{2+}. In minerals with Ca < 4 apfu (e.g. raslakite or sergevanite, Chukanov *et al.*, 2003, 2020), Ca alternates with smaller cations in the $M1_6O_{24}$ ring which results in the division of the *M*1 site into two independent *M*1a and *M*1b sites and a change of symmetry from $R3m$ or $R\bar{3}m$ to $R3$. In Type-2 minerals, the *M*2 micro-region is commonly Fe,Mn-deficient and accumulates Na and Zr in accordance with the substitution scheme $3(Fe^{2+},Mn^{2+}) \rightarrow 2Na + Zr$. The *M*3 and *M*4 sites of the Lovozero-type eudialytes can contain significant amounts of niobium and can be Nb-dominant. The Type-2 EGM are especially typical in foyaites.

Type-3 EGM (Kovdor type) are enriched in Ca and contain 6.5 to 10 Ca apfu. Excessive calcium occurs at the *N*3 and/or *N*4 sites and, usually, significant amounts of Nb occur at the *M*3 and/or *M*4 site. High contents of carbonate anions at the *X* sites are a specific feature of the Type-3 EGM. These minerals are typical for peralkaline rocks of ultrabasic–alkaline massifs with carbonatites. Carbonatites are considered as the source of calcium and CO_3^{2-} groups (Rozenberg *et al.*, 2005; Chukanov *et al.*, 2005; Moiseev, Chukanov, 2006). In the structures of some Type-3 EGM, strontium can have the same role as calcium (Rastsvetaeva *et al.*, 2018; Gritsenko *et al.*, 2020). As a rule, Sr-rich Type-3 EGM contain significant amounts of CO_3^{2-} groups occurring at the *X* sites.

In previous work, eudialyte has been synthesised as a component of polymineral assemblages, including aegirine, vlasovite and other zirconosilicates, from a mixture with the composition $6SiO_2 + ZrO_2 + 6Na_2CO_3 + CaCO_3 + FeCl_2 + 4H_2O$ in the presence of Na_2SiF_6 or K_2SiF_6, with temperature range of 450–550°C and H_2O pressures of 85 to 700 bars (Christophe-Michel-Lévy, 1961). In that work, eudialyte was identified by powder X-ray diffraction (PXRD) data. It formed subhedral pseudohexagonal platy crystals ∼50 μm across which were almost optically isotropic, with a refractive index of 1.592. Unfortunately, no compositional data were obtained for this sample.

Recently, decomposition of eudialyte in different solvents was studied at 100°C for 48 h (Smirnova *et al.*, 2015). In particular, it was shown that in 2 to 10% hydrochloric acid complete decomposition takes place. The interaction of eudialyte with 1–7% solutions of oxalic acid results in leaching of Ca, Na and *REE*, though the zirconosilicate framework remains.

Table 1. The composition of the starting mixture.

Component	Weight (g)
SiO_2	0.90
$ZrOCl_2$	0.32
Fe_2O_3	0.14
CaO	0.19
Na_2CO_3	0.45
Total	2.0

In this work, we report the synthesis of eudialyte-type compounds which are close to the Types 1–3 but are depleted in iron.

Experimental

Starting materials

In the experiments, a mixture of Na_2CO_3, CaO, Fe_2O_3, $ZrOCl_2$, and amorphous SiO_2 obtained by deposition from tetraethyl orthosilicate solution (Trofimova *et al.*, 2011) was used (Table 1). $ZrOCl_2 \cdot 8H_2O$ was preliminarily dehydrated in an oven at a temperature of 150°C for 8 hours, and then added in the required amount to the starting mixture. This was done in order to prevent excess water in the system. Na_2CO_3 and CaO were also subjected to calcination at this temperature. The Na:Ca:Fe:Zr:Si ratio of the mixture corresponded to the eudialyte end-member $Na_{15}Ca_6Fe_3Zr_3Si(Si_{25}O_{73})(OH)Cl_2 \cdot H_2O$.

A starting mixture was prepared by gradually adding a premeasured amount of each reagent into a nitric acid solution at 200°C; Fe_2O_3 and amorphous SiO_2 were added last. The mixture was then evaporated until a slurry was formed. The mixture was then placed in alundum crucibles and calcined at 450°C at atmospheric pressure in a muffle furnace for 14 days until complete decomposition of nitrates had taken place. The resulting sol-gel was ground in jasper mortars with ethyl alcohol to improve homogeneity and was then used as a starting material. As a seed, powdered natural raslakite (a Ca-deficient member of the eudialyte group) from the Alluaiv mountain, Lovozero alkaline massif, with the empirical formula $(H_3O)_xNa_{14.03}K_{0.24}Ca_{3.34}Fe^{2+}_{2.30}Mn_{0.60}Zr_{3.23}Ti_{0.24}(Si_{0.81}Nb_{0.19})(Si_{25}O_{73})Cl_{1.08}(SO_4)_{0.12}(OH,H_2O)_n$ ($x \approx 3$, $n \approx 3$) was added in amounts of 2 wt.% of the whole charge.

Synthesis

All syntheses were carried out in high-pressure reactors with internal heating (UVGD-10000 designed in the D.S. Korzhinskii Institute of Experimental Mineralogy of the Russian Academy of Sciences). Temperature and pressure measurement accuracy was ±2°C and ±50 bar, respectively.

The starting materials (150 mg of the sol-gel and 3 mg of the seed) were placed in platinum ampoules 50 mm in length, with a diameter of 4–5 mm and wall thickness of 0.1–0.2 mm. The required amount of fluid was added, then the ampoules were sealed, weighed and tested for hermeticity.

In order to determine the role of chlorine in the formation of eudialyte, three synthesis routes, with different kinds and amounts of the fluids, were carried out: 100 ml of 1 M NaCl (Route 1), 150 ml of 1 M NaCl (Route 2) and 100 ml of 1 M NaF (Route 3). The filled ampoules were placed in the reactors and held at the required *PT* parameters (600°C and 2 kbar) for 10 days. The *PT* parameters were chosen on the basis of data from Kogarko *et al.* (2002) on the formation of eudialyte-bearing mineral assemblages of the Lovozero massif. Quenching was carried out under isobaric conditions. After the experiments, the ampoules were weighed to control if they had or had not leaked. At the conclusion of the experiment, after unloading the ampoules, the solid products were washed with distilled water and dried in an oven at a temperature of 80°C.

Research methods

Raman spectra were measured at ambient conditions in the Institute of Experimental Mineralogy RAS using apparatus consisting of a Acton SpectraPro-2500i spectrograph with detector cooling up to −70°C, CCD Pixis2K and an Olympus microscope with a continuous solid-state monomeric laser with radiation wavelength of 532 nm and diode pumping. The laser beam diameter was ~4 μm. The spectral range resolution was 3.8 cm^{-1}. Raman data were collected by repeated exposures of 480 s (4 × 120 s).

Powder X-ray diffraction data were obtained at a temperature of 25°C using a Bruker-D8 diffractometer in scanning mode with a step of 0.02° and 7–40°θ range using Co*K*α radiation (wavelength = 1.78892 Å). These data were used to determine unit-cell parameters of the synthesised eudialyte-type compounds. Spectroscopic-purity silicon with $a = 5.4307$ Å was used as an internal standard. The source-to-sample distance was ~14 cm.

To obtain infrared (IR) absorption spectra, powdered samples (~0.2 mg of each) were mixed with anhydrous KBr, pelletised, and analysed using an ALPHA FTIR spectrometer (Bruker Optics) at a resolution of 4 cm^{-1}. A total of 16 scans were collected for each spectrum. The IR spectrum of an analogous pellet of pure KBr was used as a reference.

Electron probe microanalysis, including imaging of the experimental products in secondary (SEM) and back-scattered electron (BSE) modes were performed locally (D.S. Korzhinskii Institute of Experimental Mineralogy the Russian Academy of Sciences) using a Tescan VEGA-II XMU analytical suite including a digital scanning electron microscope with an energy-dispersive spectrometer (EDS) INCA Energy 450 and semiconducting Si (Li) detector Link INCA Energy and wave-dispersive spectrometer (WDS) Oxford INCA Wave 700; (produced by Tescan Orsay Hld., Brno, Czech Republic, https://www.tescan.com). The SEM is equipped with YAG (Y-Al garnet) secondary and back-scattered electron detectors. Calculations of the results of microanalysis were made using INCA *Microanalysis Suite 4.15* (version 18d+SP4) with an option for accounting for possible matrix effects from WDS analysis. The analyses were performed using an accelerating voltage of 20 kV. The current of the absorbed electrons on a reference sample of cobalt was 195–210 pA and the current of the polished samples varied from 110 to 200 pA depending on the microrelief, structure and composition of the samples. The spectra acquisition time was 100 s. The sample-to-detector distance was 25 mm. The size of an electronic 'spot' on the surface of a sample varied in the range of 157–180 nm, and the zone of excitation was ~4–5 μm. To check for Na migration during the analysis, additional measurements with a beam defocused to the area of 20 × 20 μm were made. The following standards and analytical lines were used: CaF_2 (F*K*α); albite (Na*K*α); wollastonite (Ca*K*α); synthetic Al_2O_3 (Al*K*α); SiO_2 (Si*K*α); pure Fe (Fe*K*α); pure Zr (Zr*L*α); pure Hf (Hf*L*α); and synthetic NaCl (Cl*K*α).

Results

Composition and morphological features of the products

The products obtained during the experiments are fine-crystalline aggregates of greenish-beige colour. In BSE images (Figs 1 and 2), well-formed hexagonal crystals of newly-formed eudialyte-type compounds can be seen. The main crystal forms are pinacoid {0001}, prism $\{11\bar{2}0\}$ and rhombohedron $\{02\bar{2}1\}$.

Compositional data are given in Table 2. The product obtained in Route 1 is close to Type-1 EGM (Khibiny type) based on the Ca content although unlike typical Type-1 EGM, it is Fe-deficient and enriched in Zr. Taking into account the general crystal-chemical regularities for EGM, one can conclude that in the crystal structure of this compound the *M*2 site has a mixed occupancy (Fe + Zr + Na).

For the EGM obtained by Route 2, two groups of local compositions with contrasting Ca and Fe contents can be distinguished. They correspond to a Ca-rich and Fe-deficient eudialyte variety (Route 2a) and Fe-deficient Nb-free analogue of golyshevite (Route 2b). Thus, these products are intermediate between the Fe-deficient analogues of Type 1 and Type 3.

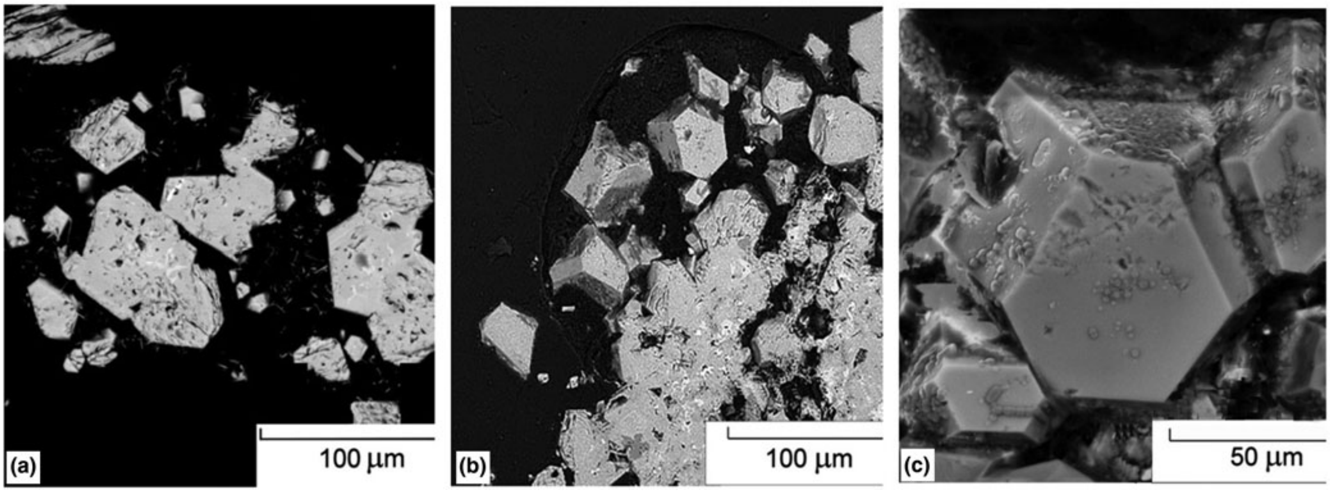

Fig. 1. BSE (BSE+SE combined in (c)) images of crystals of synthesised eudialyte-related compounds: (a) Route 1 (polished section, from experiment #23), (b) Route 2a and (c) Route 2b (samples from experiment #24).

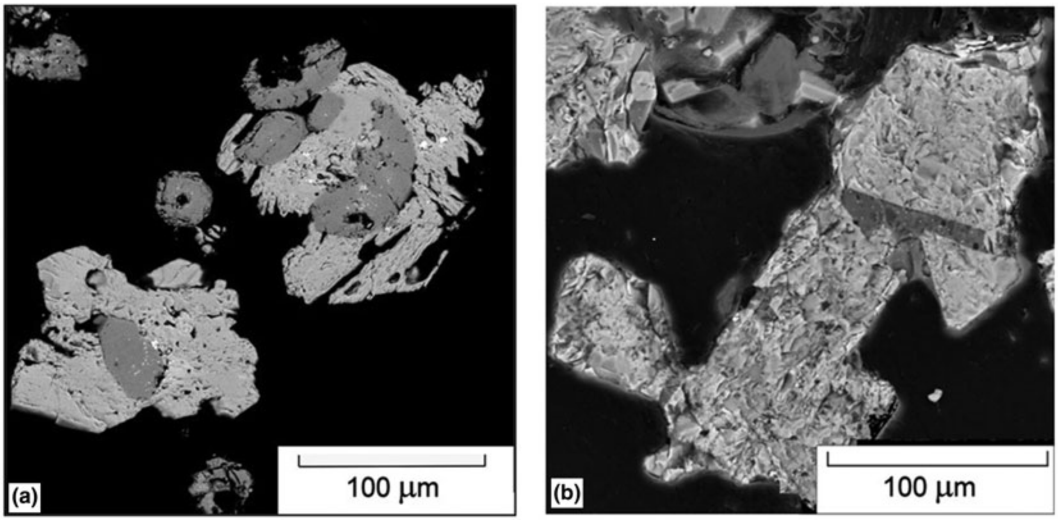

Fig. 2. BSE (BSE+SE combined in (b)) images of polished sections of the products obtained in Route 3: (a) eudialyte-type compound (light grey) and lalondeite (dark grey) and (b) crystals of a eudialyte-type compound (light grey) with aegirine inclusions (dark grey) (samples from experiment #25).

The eudialyte-related compound obtained in Route 3 corresponds to Type 2 (Lovozero type). It is Ca-and Fe-deficient and contains an excess of Zr (1.02 apfu) compared to the eudialyte end-member. In addition, this product is Na rich, which is also a specific feature of Type-2 EGM.

Infrared spectroscopy

Absorption bands in the IR spectra of eudialyte-related compounds obtained in the Routes 1 to 3 are shown in Fig. 3. The assignment of bands, based on the analysis of IR spectra of several tens of structurally investigated eudialyte-group minerals in accordance with Rastsvetaeva *et al.* (2012) is as follows: 3400 to 3700 cm^{-1} is assigned to O–H stretching vibrations; 1630 to 1650 cm^{-1} to H–O–H bending vibrations; 1430 to 1510 cm^{-1} to the asymmetric stretching mode of carbonate groups situated at the X sites; 900 to 1100 cm^{-1} to Si–O stretching vibrations; 737 to 740 cm^{-1} to mixed vibrations of rings of SiO_4 tetrahedra ('ring band': Sitarz *et al.*, 2000); 640 to 700 cm^{-1} to other mixed modes of the rings of SiO_4 tetrahedra; and 527 to 530 cm^{-1} to (Zr,Fe)–O stretching vibrations. Bands below 500 cm^{-1} correspond to lattice modes involving predominantly bending vibrations of rings of SiO_4 tetrahedra and Ca–O stretching vibrations.

Table 2. Composition (wt.%) of the synthesised eudialyte-type compounds (S.D. = standard deviation; bdl = 'below detection limit').

Component	Route 1		Route 2a		Route 2b		Route 3	
	Content	S.D.	Content	S.D.	Content	S.D.	Content	S.D.
SiO_2	52.35	1.08	51.37	0.37	51.25	0.38	53.26	0.99
ZrO_2	15.85	1.49	13.63	0.76	13.03	1.17	16.87	1.48
HfO_2	0.06	0.13	0.35	0.36	0.10	0.19	0.17	0.25
FeO	2.88	0.40	3.74	0.33	2.48	0.78	2.26	0.48
CaO	10.77	2.01	13.20	0.57	16.17	0.46	9.10	0.64
Na_2O	14.76	0.54	12.95	1.04	13.37	0.30	15.59	0.65
Cl	0.99	0.25	1.03	0.20	1.15	0.16	0.27	0.20
F	bdl	–	bdl	–	bdl	–	0.79	0.29
–O=(Cl,F)	–0.22	0.06	–0.23	0.04	–0.26	0.04	–0.39	0.04
Total	97.43		96.02		97.29		97.93	
Structural formulae calculated on the basis 26 atoms of Si								
Si	26.00		26.00		26.00		26.00	
Zr	3.84		3.37		3.22		4.02	
Hf	0.01		0.03		0.01		0.02	
Fe	1.20		1.58		1.05		0.92	
Ca	5.72		7.16		8.78		4.76	
Na	14.20		12.70		13.16		14.76	
Cl	0.83		0.88		0.99		0.23	
F	0.00		0.00		0.00		1.02	

Note: The compositional data are averaged over four (in Routes 1, 2b, and 3) or two (for Route 2a) spot analyses.

Low intensities of the bands at 527–530 cm^{-1} (Routes 1 to 3) and high intensities of the peaks at 938 and 944 cm^{-1} (Routes 1 and 2) reflect low contents of iron at the $M2$ site and high occupancies of the $M3$ and $M4$ sites with Si. A relatively low intensity of the peak at 940 cm^{-1} in the IR spectrum of the product obtained in Route 3 might indicate the presence of vacancies at the $M3$ and $M4$ sites (Rastsvetaeva *et al.*, 2012).

According to the IR spectroscopy data, all eudialyte-related compounds obtained in this work contain carbonate groups. Clearly Na_2CO_3 was the source of these carbonate-group bands. However, the product obtained in Route 3 is characterised by a low CO_3^{2-} content, which is typical for the Type-2 EGM.

Raman spectroscopy

The Raman spectra of the seed (natural raslakite) and the eudialyte-related compound obtained in Route 2 are shown in Fig. 4. Both spectra contain bands of stretching vibrations of Si–O–Si and Si–O–Zr fragments (in the ranges of 990–1090 and 520–570 cm^{-1}, respectively) and apical Si–O bonds (940–970 cm^{-1}) as well as mixed and bending vibrations of the heteropolyhedral framework (other bands below 870 cm^{-1}). Bands in the range of 1200 to 3200 cm^{-1} correspond to strong hydrogen bonds in hydrated H_3O^+ complexes (Zundel and Eigen cations) with the O···O distances from 2.38 to 2.72 Å, which are very typical components of Na-depleted eudialyte-group minerals (Chukanov *et al.*, 2022).

X-ray diffraction

Data from PXRD for the synthesised materials are given in Table 3. These data, show that the products of Route 1 and

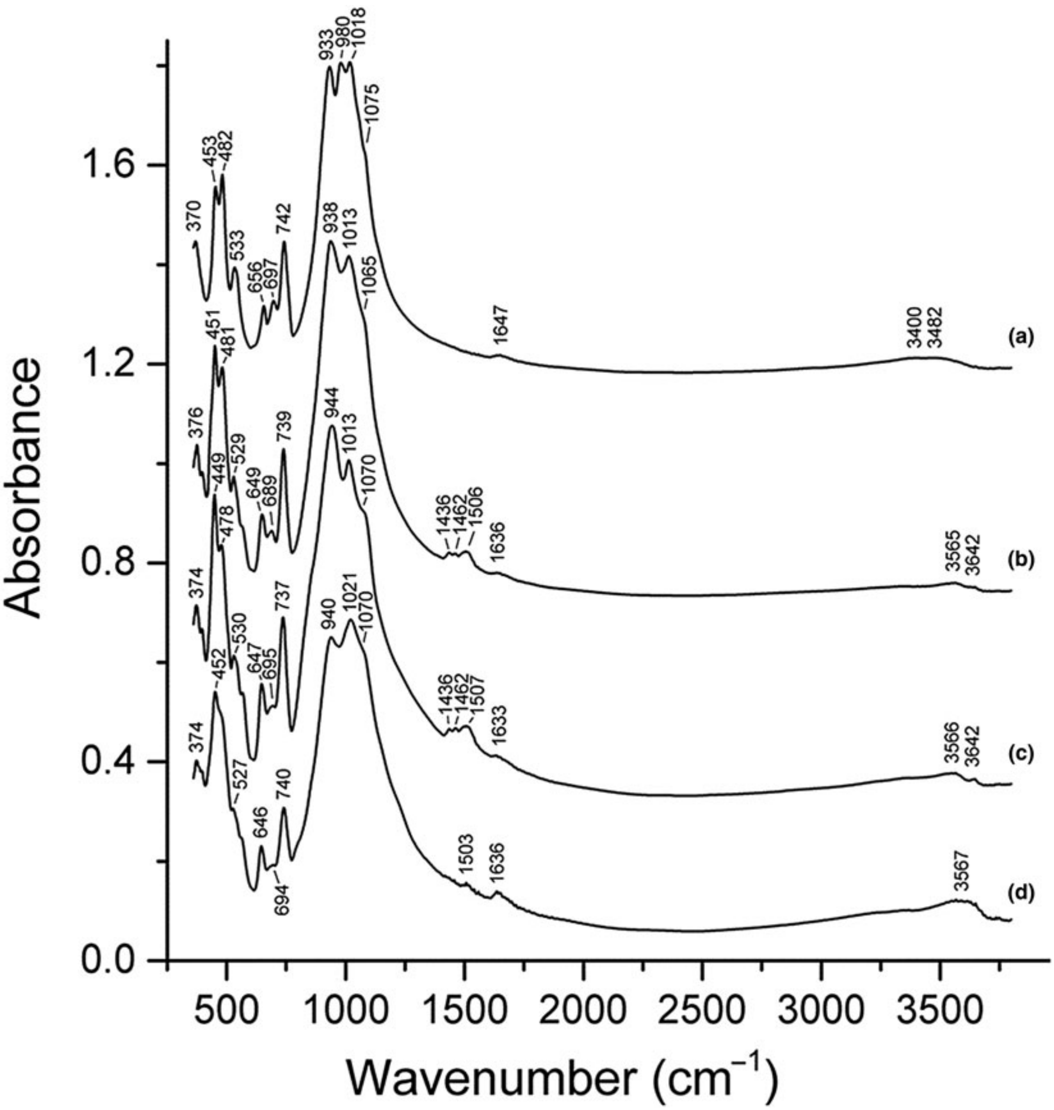

Fig. 3. Infrared absorption spectra of the seed used in the syntheses (a) and eudialyte-related compounds obtained in Route 1 (b), Route 2 (c), and Route 3 (d).

Route 2 are almost pure eudialyte-type compounds whereas the product of Route 3 contains significant amounts of impurities, including lalondeite $(Na,Ca)_6(Ca,Na)_3Si_{16}O_{38}(F,OH)_2{\cdot}3H_2O$, vlasovite $Na_2ZrSi_4O_{11}$ and Ca-bearing aegirine $(Na,Ca)(Fe^{3+},Fe^{2+})Si_2O_6$. Other (minor) impurities detected by semiquantitative EDS analysis are pectolite and an unidentified, presumably X-ray amorphous zirconosilicate forming fine intergrowths with vlasovite. Impurity peaks at 2.999 and 2.995 Å observed in the PXRD patterns of the products of Route 1 and Route 2, respectively, might correspond to the -OH analogue of lalondeite $(Na,Ca)_6(Ca,Na)_3Si_{16}O_{38}(OH)_2{\cdot}3H_2O$.

Discussion

Preliminary syntheses in the Na–Ca–Zr–Nb–Fe–Mn–Si–O–(Cl,F) system, which were previously conducted by us (2019–2021), were carried out at different *P*–*T* conditions (temperature 450–600°C and pressure 1.5–2.5 kbar) with wide ranges of compositions and different fluids (1 M solutions of NaCl, NaF, or NaOH and including high-alkaline fluids, 20 and 40% NaOH), both with and without a seed. These experiments showed that for the crystallisation of eudialyte-type compounds in these systems the presence of both a seed and Cl^- or F^- ions is necessary. In the presence of high-alkaline fluids, other zirconosilicates (parakeldyshite and/or zirsinalite) are formed. This observation is in agreement with the replacement of eudialyte-group minerals with parakeldyshite or zirsinalite at the peralkaline hyperagpaitic stages of the evolution of the igneous rocks and pegmatites of the Lovozero and Khibiny massifs (Khomyakov, 1995). Under hydrothermal conditions, EGM can be either pseudomorphed or dissolved. Alteration of eudialyte was observed at 230°C and pH below 10.5 (Mikhailova *et al.*, 2022). The dissolution process was most intensive in acidic hydrothermal solutions. Thus, EGM are stable only under high-alkaline conditions and data obtained in this work confirm this conclusion.

All eudialyte-related compounds synthesised in this work are Fe deficient compared to eudialyte *s.s.* This observation could be related partly to the crystallisation of acicular aegirine as a

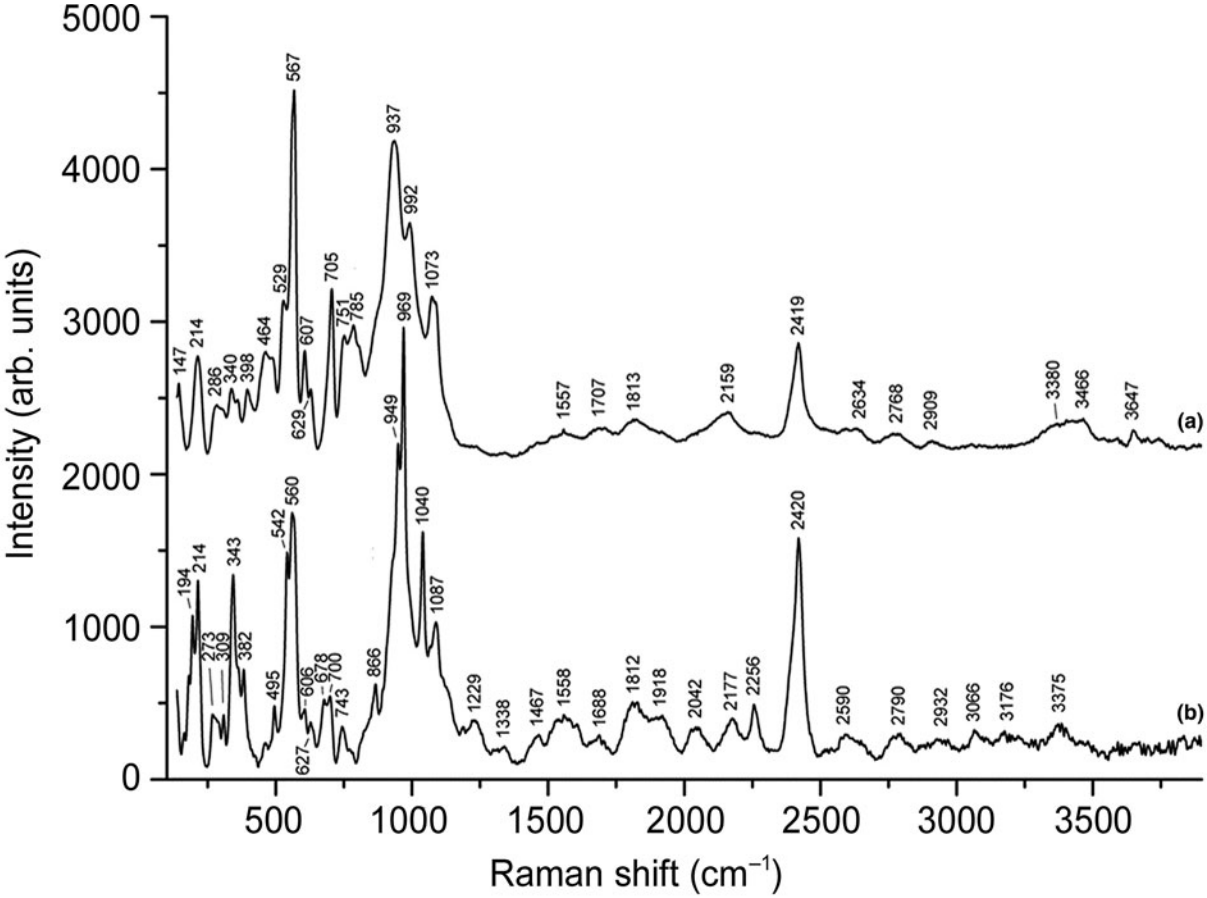

Fig. 4. Raman spectra of the seed used in the syntheses (a) and the eudialyte-related compound obtained in Route 2 (b).

minor impurity in all syntheses products. Another possible cause of low Fe contents in the synthesised eudialyte-related compounds could be the low solubility of Fe_2O_3.

To date, the crystal structures of more than 100 samples of minerals belonging to the eudialyte group have been characterised, which makes it possible to elucidate the predominant regularities in the distribution of diverse elements between different sites in their crystal structures (Johnsen *et al.*, 2003; Rastsvetaeva *et al.*, 2012, 2020, Rastsvetaeva and Chukanov, 2020). On the basis of these regularities, the crystal-chemical formulae of the synthesised eudialyte-type compounds can be written as follows:

$Na_{13.89-x}(H_3O)_y(Ca_{5.72}Na_{0.28})(Fe_{1.20}Zr_{0.95}Na_x)(Zr_{2.99}Hf_{0.01})Si_2(Si_{24}O_{72})(O,OH,CO_3)_zCl_{0.83}\cdot nH_2O$ (Route 1);

$(Na_{12.70-x}Ca_{1.16})Ca_6(Fe_{1.58}Zr_{0.40}Na_x)(Zr_{2.97}Hf_{0.03})Si_2(Si_{24}O_{72})(O,OH)_y(CO_3)_zCl_{0.88}\cdot n(H_2O,H_3O)$ (Route 2a);

$(Na_{13.16-x}Ca_{2.78})Ca_6(Fe_{1.05}Zr_{0.23}Na_x)(Zr_{2.99}Hf_{0.01})Si_2(Si_{24}O_{72})(O,OH)_yCl_{0.99}(CO_3)_z\cdot n(H_2O,H_3O)$ (Route 2b);

$Na_{13.52-x}(Ca_{4.76}Na_{1.24})(Fe_{0.92}Zr_{1.04}Na_x)(Zr_{2.98}Hf_{0.02})Si_2(Si_{24}O_{72})(O,OH)_yF_{1.02}\cdot n(H_2O,H_3O)$ (Route 3).

As a rule, the enhanced *c* parameter of ~31 Å corresponds to H_3O-rich eudialyte-group minerals. The product of Route 1 has a *c* parameter of 30.934 Å which might be an indirect indication of a high H_3O:H_2O ratio in this compound compared to other eudialyte-related compounds synthesised in this work.

According to IR spectroscopy data, all synthesised eudialyte-related compounds belong to high-silicon (i.e. with a low vacancy content at the *M*3 and *M*4 sites) and Fe-deficient types. The first two formulae correspond to an Fe-deficient variety of eudialyte *s.s.*, in which Fe that should dominate at the *M*2 site is mostly replaced by Zr and Na. The other two formulae (Route 2b and Route 3) do not correspond to any known mineral species belonging to the eudialyte group.

The product with the highest Ca content (Route 2b) is associated with golyshevite $(Na,Ca)_{10}Ca_9Fe_2Zr_3NbSi_{25}O_{72}(OH)_3(CO_3)\cdot H_2O$ (Chukanov *et al.*, 2005), from which it differs in the absence of Nb and a low Fe content. By analogy with golyshevite, it can be assumed that in this compound, Ca in excess of 6 apfu is concentrated at the *N*4 site. As can be seen from the compositional data, the product of Route 3 is characterised by the highest content of impurity phases, among which lalondeite, vlasovite and aegirine are identified (Table 3). The formation of lalondeite is associated with the presence of fluorine in the fluid phase used in Route 3. During the crystallisation of lalondeite and aegirine, the stoichiometry of the mineral-forming medium changes. In particular, the Zr:Si ratio increases, which promotes the crystallisation of vlasovite.

As a rule, natural minerals of the eudialyte group are characterised by low fluorine contents: even in samples from the paragenesis with villiaumite NaF, chlorine, as a rule, dominates over fluorine. The only F-dominant EGM is kentbrooksite $(Na,\mathit{REE})_{15}(Ca,\mathit{REE})_6Mn_3Zr_3[SiNb](Si_{24}O_{74})F_2\cdot 2H_2O$ (Johnsen *et al.*, 1998). It is very probable that chlorine is a component that

Table 3. The strongest reflections in the powder X-diffraction patterns of the products of Routes 1 to 3.

d, Å (*I*, %)			
Route 1	Route 2	Route 3	*hkl* and/or impurity
		11.91 (42)	Lalondeite
7.13 (29)	7.14 (41)	7.10 (38)	110
6.47 (18)	6.48 (25)	6.48 (38)	104
	6.43 (18)	6.38 (32)	Aegirine
6.05 (15)	6.06 (21)	6.03 (25)	021
		5.95 (61)	Lalondeite
5.72 (23)	5.73 (27)	5.70 (26)	202
		5.43 (18)	Vlasovite
		5.05 (70)	Vlasovite
		4.42 (30)	Aegirine
4.33 (60)	4.33 (75)	4.32 (71)	205
4.12 (22)	4.13 (30)	4.12 (26)	116
4.09 (17)	4.11 (22)	4.10 (19)	300
3.98 (20)	3.97 (20)	3.97 (61)	$\bar{2}34$ (+ lalondeite)
		3.866 (30)	Vlasovite
3.810 (32)	3.808 (39)	3.799 (37)	033
		3.658 (25)	Lalondeite
3.554 (39)	3.552 (36)	3.548 (54)	220, 027
3.403 (36)	3.402 (25)	3.390 (26)	131
3.342 (25)	3.348 (27)	3.342 (40)	$\bar{3}42$
		3.249 (26)	Vlasovite
3.235 (34)	3.233 (40)	3.234 (65)	208
3.181 (27)	3.177 (39)	3.190 (37), 3.164 (46)	217
3.052 (23)	3.051 (22)	3.059 (33)	$\bar{1}29$
2.999 (33)	2.995 (36)		Unidentified impurity
		2.989 (77)	Lalondeite + aegirine
2.982 (92)	2.981 (91)	2.973 (100)	$\bar{3}45$
		2.945 (26)	Vlasovite
2.917 (23), 2.909 (20)	2.915 (28), 2.906 (20)	2.907 (53)	$\bar{2}46$ (+aegirine)
2.858 (100)	2.854 (100)	2.850 (83)	404
2.688 (26)	2.687 (23)	2.687 (20)	137
2.609 (33)	2.606 (28)	2.607 (30)	309
2.532 (19)	2.533 (18)	2.547 (19), 2.528 (26)	0.0.12
2.487 (17)		2.483 (20)	Aegirine
2.164 (21)	2.161 (19)	2.163 (22)	4.0.10
		1.984 (17)	Lalondeite
1.780 (31)	1.780 (18)	1.775 (21)	4.2.11, 440, 0.4.14
Refined unit-cell parameters			
a = 14.238(3) Å	14.238(3) Å	14.198(3) Å	
c = 30.934(11) Å	30.377(9) Å	30.364(9) Å	
V = 5335(4) Å^3	5333(4) Å^3	5301(4) Å^3	

stabilises the structure of eudialyte. This assumption is consistent with the formation of a large amount of by-products in Route 3.

Acknowledgements. This work has been carried out in accordance with the state task, state registration numbers AAAA-A19–119092390076–7 (analytical data processing and IR spectroscopy) and FMUF–2022–0002 (the rest of the work).

Competing interests. The authors declare none.

References

Christophe-Michel-Lévy M. (1961) Reproduction artificielle de quelques minéraux riches en zirconium (zircon, eudialyte, catapléite, elpidite); comparaison avec leurs conditions naturelles de formation. *Bulletin de la Société Française de Minéralogie et de Cristallographie*, **84**, 3, 265–269, https://doi.org/10.3406/bulmi.1961.5487.

Chukanov N.V., Pekov I.V., Zadov A.E., Korovushkin V.V., Ekimenkova I.A. and Rastsvetaeva R.K. (2003) Ikranite, $(Na,H_3O)_{15}(Ca,Mn,REE)_6Fe^{3+}_2Zr_3(\square,Zr)(\square,Si)Si_{24}O_{66}(O,OH)_6Cl{\cdot}nH_2O$, and raslakite, $Na_{15}Ca_3Fe_3(Na,Zr)_3Zr_3(Si,Nb)(Si_{25}O_{73})(OH,H_2O)_3(Cl,OH)$, new eudialyte-group minerals from the Lovizero massif. *Zapiski Rossiiskogo Mineralogicheskogo Obshchestva* (*Proceedings of the Russian Mineralogical Society*), **132**, 5, 22–33 [in Russian].

Chukanov N.V., Moiseev M.M., Rastsvetaeva R.K., Rozenberg K.A., Zadov A.E., Pekov I.V. and Korovushkin V.V. (2005) Golyshevite $(Na,Ca)_{10}Ca_9Fe_2Zr_3NbSi_{25}O_{72}(OH)_3(CO_3){\cdot}H_2O$ and mogovidite $Na_9(Ca,Na)_6Ca_6Fe_2Zr_3\square Si_{25}O_{72}(CO_3)(OH,H_2O)_4$ – new eudialyte-group minerals from hypercalcium pegmatites of Kovdor. *Zapiski VMO* (*Proceedings of the Russian Mineralogist Society*), **134**, 6, 36–46 [in Russian].

Chukanov N.V., Aksenov S.M., Pekov I.V., Belakovskiy D.I., Vozchikova S.A. and Britvin S.N. (2020) Sergevanite, $Na_{15}(Ca_3Mn_3)(Na_2Fe)Zr_3Si_{26}O_{72}(OH)_3{\cdot}H_2O$, a new eudialyte-group mineral from the Lovozero alkaline massif, Kola Peninsula. *The Canadian Mineralogist*, **58**, 421–436, https://doi.org/10.3749/canmin.2000006.

Chukanov N.V., Vigasina M.F., Rastsvetaeva R.K., Aksenov S.M., Mikhailova Ju.A. and Pekov I.V. (2022) The evidence of hydrated proton in eudialyte-group minerals based on Raman spectroscopy data. *Journal of Raman Spectroscopy*, **53**, 1188–1203, https://doi.org/10.1002/jrs.6343.

Gritsenko Y.D., Chukanov N.V., Aksenov S.M., Pekov I.V., Varlamov D.A., Pautov L.A., Vozchikova S.A., Ksenofontov D.A. and Britvin S.N. (2020) Odikhinchaite, $Na_9Sr_3[(H_2O)_2Na]Ca_6Mn_3Zr_3NbSi(Si_{24}O_{72})O(OH)_3(CO_3){\cdot}H_2O$, a new eudialyte-group mineral from the Odikhincha intrusion, Taimyr Peninsula, Russia. *Minerals*, **10**, 1062, https://doi.org/10.3390/min10121062.

Johnsen O., Grice J.D. and Gault A. (1998) Kentbrooksite from the Kangerdlugssuaq intrusion, East Greenland, a new Mn-*REE*-Nb-F end-member in a series within the eudialyte group: Description and crystal structure. *European Journal of Mineralogy*, **10**, 207–219, https://doi.org/10.1127/ejm/10/2/0207.

Johnsen O., Ferraris G., Gault R.A., Grice J.D., Kampf A.R. and Pekov I.V. (2003) Nomenclature of eudialyte-group minerals. *The Canadian Mineralogist*, **41**, 785–794, https://doi.org/10.2113/gscanmin.41.3.785.

Khomyakov A.P. (1995) *Mineralogy of Hyperagpaitic Alkaline Rocks*. Clarendon Press, Oxford, 223 pp.

Kogarko L.N., Williams C.T. and Wooley A.R. (2002) chemical evolution and petrogenetic implications of loparite in the layered, Agpaitic Lovozero Complex, Kola Peninsula, Russia. *Mineralogy and Petrology*, **74**, 1–24, https://doi.org/10.1007/s710-002-8213-2.

Mikhailova Yu.A, Pakhomovsky Ya.A., Kalashnikova G.O. and Aksenov S.M. (2022) Dissolution of the eudialyte-group minerals: Experimental modeling of natural processes. *Minerals*, **12**, 1460, https://doi.org/10.3390/min12111460.

Moiseev M.M. and Chukanov N.V. (2006) Mineralogy of alkaline pegmatites and hydrothermalites of the Kovdor massif. *New Data on Minerals*, **41**, 56–70.

Rastsvetaeva R.K. and Chukanov N.V. (2020) New data on the isomorphism in eudialyte-group minerals. 2. Crystal-chemical mechanisms of blocky isomorphism at the key sites (a review). *Minerals*, **10**, 720, https://doi.org/10.3390/min10080720.

Rastsvetaeva R.K., Chukanov N.V. and Aksenov S.M. (2012) *Eudialyte-Group Minerals*. Nizhny Novgorod State University, Nizhny Novgorod, Russia, 230 pp. [in Russian].

Rastsvetaeva R.K., Chukanov N.V., Zaitsev V.A., Aksenov S.M. and Viktorova K.A. (2018) Crystal structure of Cl-deficient analogue of taseqite from Odikhincha Massif. *Crystallography Reports*, **63**, 349–357, https://doi.org/10.1134/S1063774518030240.

Rastsvetaeva R.K., Chukanov N.V., Pekov I.V., Schäfer Ch. and Van K.V. (2020) New data on the isomorphism in eudialyte-group minerals. 1. Crystal chemistry of eudialyte-group members with Na incorporated into the framework as a marker of hyperagpaitic conditions. *Minerals*, **10**, 87–102, https://doi.org/10.3390/min10070587.

Rozenberg K.A., Rastsvetaeva R.K., Chukanov N.V. and Verin I.A. (2005) Crystal structure of golyshevite. *Crystallography Reports*, **50**, 539–543, https://doi.org/10.1134/1.1996727.

Sitarz M., Handke M. and Mozgawa W. (2000) Identification of silicooxygen rings in SiO_2 based on IR spectra. *Spectrochimica Acta A*, **56**, 9, 1819–1823, https://doi.org/10.1016/S1386-1425(00)00241-9.

Smirnova T.N., Pekov I.V., Varlamov D.A., Kovalskaya T.N., Bychkov A.Yu. and Bychkova Ya.V. (2015) On the chemistry and stages of phase formation processes during the acid decomposition of eudialyte (according to experimental data). Pp. 167–170 in: *Ontogeny, Phylogeny, System of Mineralogy*. Materials of the All-Russian Conference, Miass, Russia [in Russian].

Trofimova E.Yu., Aleksenskii A.E., Grudinkin S.A., Korkin I.V., Kurdyukov D.A. and Golubev V.G. (2011) Effect of tetraethoxysilane pretreatment on synthesis of colloidal particles of amorphous silicon dioxide. *Colloid Journal*, **73**, 546–550, https://doi.org/10.1134/s1061933×11040156.